

## Cerium-based nanoparticles for cancer photodynamic therapy

Hui Li\*, Min Wei\*, Xinyi Lv\*, Yanling Hu\*, Jinjun Shao\*,  
Xuejiao Song\*, Dongliang Yang\*<sup>¶,\*\*\*</sup>, Wenjun Wang<sup>†</sup>,  
Buhong Li<sup>‡</sup> and Xiaochen Dong\*<sup>§,||,\*\*\*</sup>

*\*Key Laboratory of Flexible Electronics (KLOFE) and  
Institute of Advanced Materials (IAM) School of Physical and  
Mathematical Sciences, Nanjing Tech University (NanjingTech)  
Nanjing, Jiangsu 211816, P. R. China*

*†School of Physical Science and Information Technology  
Liaocheng University, Liaocheng, Shandong 252059, P. R. China*

*‡MOE Key Laboratory of OptoElectronic Science and  
Technology for Medicine Fujian Provincial Key Laboratory of  
Photonics Technology  
Fujian Normal University, Fuzhou, Fujian 350117, P. R. China*

*§School of Chemistry & Materials Science  
Jiangsu Normal University, Xuzhou  
Jiangsu 221116, P. R. China*

*¶yangdl1023@njtech.edu.cn*

*||iamxcdong@njtech.edu.cn*

Received 9 May 2022

Accepted 24 August 2022

Published 14 October 2022

Metal- and metal-oxide-based nanoparticles have been widely exploited in cancer photodynamic therapy (PDT). Among these materials, cerium-based nanoparticles have drawn extensive attention due to their superior biosafety and distinctive physicochemical properties, especially the reversible transition between the valence states of Ce(III) and Ce(IV). In this review, the recent advances in the use of cerium-based nanoparticles as novel photosensitizers for cancer PDT are discussed, and the activation mechanisms for electron transfer to generate singlet oxygen are presented. In addition, the types of cerium-based nanoparticles used for PDT of cancer are summarized. Finally, the challenges and prospects of clinical translations of cerium-based nanoparticles are briefly addressed.

*Keywords:* Photodynamic therapy; photosensitizer; cerium; reactive oxygen species.

\*\*Corresponding authors.

## 1. Introduction

Cancer is a life-threatening disease with an incidence that increases significantly with age, resulting in the deaths of millions of people.<sup>1</sup> Conventional therapy, including surgery, chemotherapy, and radiotherapy,<sup>2</sup> can efficaciously treat some cancers and inhibit cancer metastasis. Nevertheless, these treatments have inevitable drawbacks, such as a high recurrence rate for surgical resection and severe damage to the whole body from chemotherapy and ionizing radiation. Photodynamic therapy (PDT) is a phototherapy technique that takes advantage of light sources to selectively eliminate primary and recurrent cancers,<sup>3</sup> thereby avoiding damage to normal tissue, achieving noninvasive treatment, and improving the quality of life of patients.<sup>4</sup> PDT has been gradually applied in different fields of biotechnology over the past few years because of its high efficiency, high selectivity, and noninvasiveness.<sup>5-7</sup>

PDT is a local therapeutic modality that is implemented via photoelectron energy transfer and conversion.<sup>8</sup> Under excitation by an appropriate light source, a photosensitizer (PS) interacts with oxygen to generate cytotoxic reactive oxygen species (ROS) for the treatment of various diseases. During this process, the conversion of triplet oxygen molecules ( $^3\text{O}_2$ ) into singlet oxygen ( $^1\text{O}_2$ ) is accompanied by oxygen consumption. The production of ROS by a PS can efficaciously and precisely destroy malignant tissues with minor side effects.<sup>9-11</sup>

With the continuous development of nanoscience, nanotechnology has been widely used for biomedical applications, such as in drug delivery, imaging, and biological detection, which has significantly revolutionized biomedical technology.<sup>12-14</sup> Recently, metal-based nanoparticles (NPs), such as manganese dioxide,<sup>15,16</sup> iron oxide,<sup>17</sup> and cerium oxide,<sup>18</sup> have been widely boosted for PDT with therapeutic effects.<sup>1,19</sup> In general, ideal PSs for PDT have outstanding photodynamic properties along with low or even no toxicity toward normal cells in the absence of light irradiation.<sup>20,21</sup> Among these PSs, cerium and its oxidant-based nanoparticles have received extensive attention because of its low cytotoxicity and unique physicochemical characteristics,<sup>22</sup> especially the reversible transition between the valence states of Ce(III) and Ce(IV).<sup>23</sup>

The ion diagram of  $\text{CeO}_2$  (Fig. 1) depicts the tetrahedron of Ce atoms centered on the O atom as

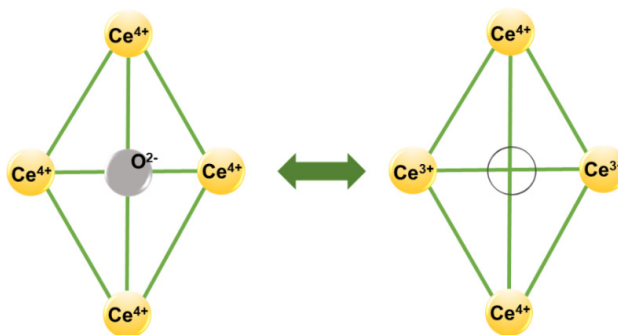


Fig. 1. Diagrammatic representation of charge redistribution that occurs after the oxygen vacancy formation in  $\text{CeO}_2$ .

well as the charges on these atoms. In Fig. 1 (from left to right), while reducing two Ce ions to the trivalent valence state, the reduction process forms a neutral oxygen vacancy (hollow circle) in the interior of the tetrahedron. With Ce(IV) occupying the octahedral interstitial sites and  $\text{O}^{2-}$  occupying the tetrahedral interstitial sites,  $\text{CeO}_2$  exhibits a face-centered cubic (FCC) fluorite crystal structure. One of the most fundamental features of  $\text{CeO}_2$  is the production and migration of oxygen vacancies, which allows for reversible conversion between antioxidants Ce(III) and prooxidants Ce(IV). The marvelous oxygen storage properties.<sup>23</sup> of  $\text{CeO}_2$  NPs have been demonstrated in photocatalysis,<sup>24</sup> magnetic semiconductors,<sup>8</sup> and oncotherapy.<sup>25,26</sup>

$\text{CeO}_2$  NPs are one type of low-toxicity rare-earth nanoparticles<sup>27</sup> that have attracted extensive attention in the field of biomedicine because of multi-enzyme mimicking activities.<sup>28</sup> In general, the PDT properties of nanoparticles are highly dependent on their structures and physicochemical properties. Chemical doping, surface functionalization, and other strategies have been utilized for modulating the physicochemical properties and morphology of  $\text{CeO}_2$  NPs to enhance photodynamic performance.

Herein, we summarize advances in the applications of cerium and its oxidant-based nanoparticles to cancer PDT (Fig. 2). The underlying working mechanisms of Ce-based PDT were first revealed with representative examples. Next, we focus on the design and synthesis of cerium-based nanoparticles. Finally, the challenges and prospects of cerium and cerium-oxide-based materials for PDT are presented.

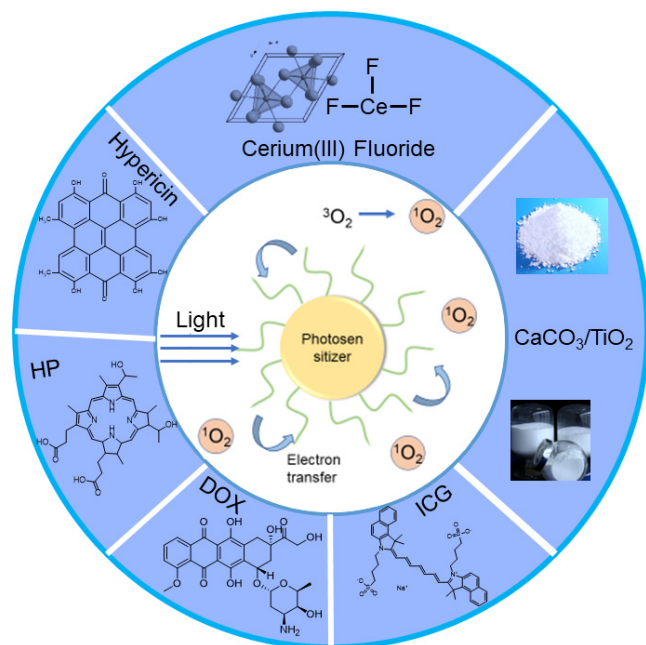


Fig. 2. Cerium-based hybrid nanoparticles for cancer PDT.

## 2. Therapeutic Mechanism of Cerium-Based Nanoparticles

Cerium-based nanoparticles have a unique mechanism for conversion between valence states and have therefore been verified as effective and durable anticancer agents.<sup>29,30</sup> PSs based on cerium and its oxidant-based nanoparticles have received considerable attention, and numerous studies have confirmed that cerium-based nanoparticles can be used for oncotherapy,<sup>31</sup> as will be discussed in detail later. A schematic of the PDT mechanism of cerium-based nanoparticles is shown in Fig. 3.

PS absorbs photon energy and then is activated, transitioning from the electronic ground state to the

excited state.<sup>32</sup> The excited PS reaches the  $T_1$ -state through the intersystem crossing and then generates ROS through electron transfer and energy transfer.<sup>33</sup> ROS include  $^1O_2$ , superoxide ions ( $\bullet O_2^-$ ), hydroxyl radicals ( $\bullet OH$ ), etc. that can cause lipid peroxidation or protein inactivation and result in cell necrosis or apoptosis [Fig. 3(a)]. Figure 3(b) shows that a PS absorbs photon energy to reach the  $S_n$ -state and then returns to  $S_1$  through internal conversion and vibrational relaxation. In this case, the excited state of PSs may undergo different experiences: intersystem crossover to the triplet excited state ( $T_1$ ) by changing the electron spin orientation, decay to the ground state to produce fluorescence, or vibration relaxation to generate heat.<sup>34,35</sup> Following intersystem crossing, molecular PSs in the  $T_1$ -state can either exhibit PDT effects by interacting with adjacent triplet state molecules, in particular with triplet oxygen ( $^3O_2$ ), to produce ROS, or they can return to the ground state by emitting phosphorescence.<sup>1</sup>

As one of the most significant functional rare-earth nanomaterial,  $CeO_2$  with ample oxygen vacancies and defects possesses a high potential to improve photocatalytic capability, thereby increasing the generation of ROS,<sup>36</sup> which provides a chance for PDT in cancer therapy. Oxidative damage is the most direct manifestation of PDT.<sup>36</sup> Generally, the oxidative stress induced by the PDT-generated ROS can be exacerbated because ROS production can be promoted by reversible conversion between antioxidants Ce(III) and prooxidants Ce(IV). *In-vitro* cell experiments have indicated that PDT-generated ROS interact with phospholipids, cholesterol, membrane proteins, and other biomolecules of cell components,

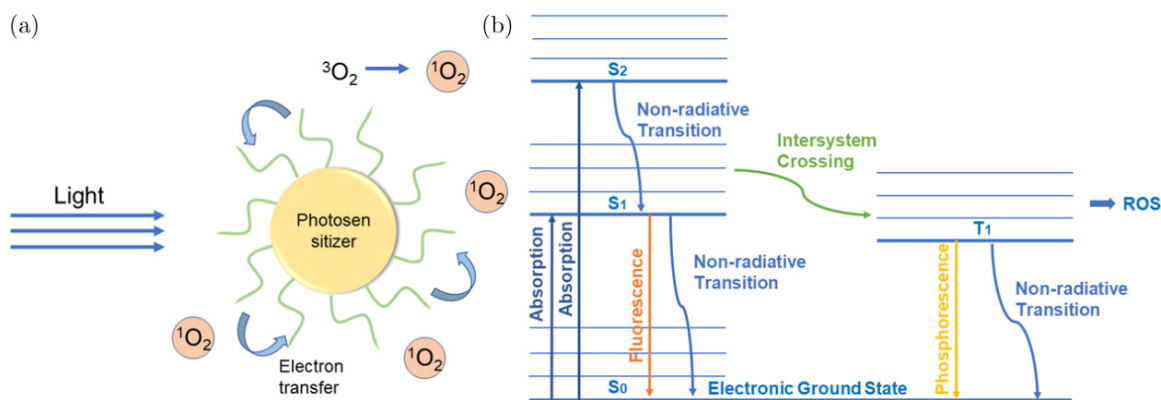


Fig. 3. (a) Cerium and its oxidant-based nanoparticles acting as PSs for electron transfer to generate  $^1O_2$ . (b) Jablonski diagram of PDT describing the excitation and relaxation process in photosensitive molecules.

resulting in the loss of cell function and even cell death.<sup>37</sup>

### 3. Compounds Containing Cerium or Cerium Oxide for PDT

With the study of cerium or cerium oxide nanoparticles, more and more cerium-based nanomaterials have been used for cancer therapy and their therapeutic mechanisms have been deciphered. In this section, we list the representative compounds containing cerium or cerium oxide that act on more than one substrate or activate under a distinct environment (Table 1).

#### 3.1. Cerium-containing compounds

The PDT effect of pure cerium-containing compounds was verified by Clement *et al.* CeF<sub>3</sub> NPs can generate <sup>1</sup>O<sub>2</sub> under irradiation by UV light or 8-keV X-rays. The <sup>1</sup>O<sub>2</sub> quantum yield of CeF<sub>3</sub> NPs was determined to evaluate the photodynamic performance. The calculated <sup>1</sup>O<sub>2</sub> generation from CeF<sub>3</sub> under X-ray exposure is 1000 ± 170, in which case the X-ray <sup>1</sup>O<sub>2</sub> quantum yield is around 0.13 ± 0.02.<sup>38</sup> The complementary mechanisms of cell death between photodynamic (membrane damage) and ionizing radiation (DNA damage) therapies are hypothesized to enable CeF<sub>3</sub> NPs to improve the radiotherapeutic effectiveness.

In 2022, Li *et al.* reported the second near-infrared region (NIR-II) light-induced nanoparticles for photoacoustic (PA) image-guided sonodynamic

amplified PDT/photothermal synergistic therapy (PTT), utilizing cerium oxide (CeO<sub>2-x</sub>) with ample oxygen vacancies (Fig. 4).<sup>39</sup> The introduction of oxygen vacancies is beneficial to minimizing the bandgap, providing a broad absorption performance in the ultraviolet–visible–NIR region for PTT. In addition, the vacancies of oxygen could allow electrons (*e*<sup>-</sup>) and holes (*h*<sup>+</sup>) to be separated from the band structure with electron trapping sites by ultrasound irradiation, promoting ROS production.<sup>40</sup> Given this, the SDT of CeO<sub>2-x</sub> is capable to amplify the effect of PDT/PTT to eliminate cancer cells. Meanwhile, the bandgap was narrowed (from 2.74 eV to 1.66 eV), allowing the absorbance of NIR laser irradiation for PDT/PTT. Oxygen vacancies could inhibit the hole–electron recombination, as well as transfer energy as heat effectively. The photogenerated electrons could catalyze molecular oxygen to generate O<sub>2</sub><sup>-•</sup>, whereas the holes in the valence band oxidized H<sub>2</sub>O to generate •OH. Besides, hyaluronic acid (HA) was coated on the surface of CeO<sub>2-x</sub> to endow it with a higher affinity for CD44 receptor overexpressed on the surface of cancer cells. This research remarkably broadened the application of NIR-II-responsive CeO<sub>2-x</sub> for PA imaging-guided SDT-enhanced PDT to the elimination of cancer cells.

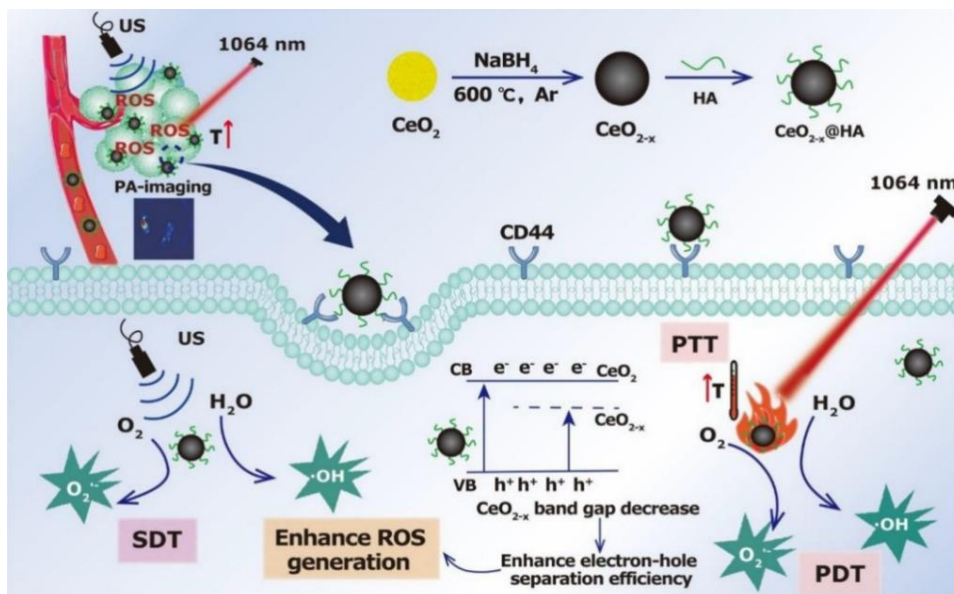
#### 3.2. Cerium/cerium-oxide-doped nanoparticles

Ionizing radiation known as X-rays interacts with molecules to produce ROS and free radicals that can

Table 1. Typical compounds containing cerium or cerium oxide for PDT.

Types of the nanomaterials	Name	Cell/tumor modal	Exogenous activators	Source
Cerium-containing compounds	CeF <sub>3</sub>	PANC-1	X-ray	Ref. 38
	CeO <sub>2-x</sub>	4T1	NIR-II	Ref. 39
Cerium/Cerium-oxide-doped nanoparticles	TiO <sub>2</sub> :Ce	A549	X-ray	Ref. 42
	Ce:CaCO <sub>3</sub>	A549	X-ray	Ref. 44
	GAG@mSiO <sub>2</sub> @RB	MDA-MB-231	X-ray	Ref. 45
	Mn <sub>x</sub> Ce <sub>1-x</sub> O <sub>2</sub>	MCF-7	630-nm laser	Ref. 46
Cerium-oxide-based inorganic composite nanoparticles	CeONR@PDA-Gal/Hyp	HepG2	590-nm laser	Ref. 51
	MSN-HP-DOX@CeO <sub>2</sub>	293 T	630-nm laser	Ref. 52
	DOX-Pt@CeO <sub>2</sub> @MnO <sub>2</sub>	HepG2	808-nm laser	Ref. 53
	ICG@PEI-PBA-HA/CeO <sub>2</sub>	MCF-7	808-nm laser	Ref. 56
	USCGP	4T1	808-nm laser	Ref. 57
Cerium-oxide-based organic composite nanoparticles	CPs	H22	808-nm laser	Ref. 58
	SPNs	4T1	808-nm laser	Ref. 62





Source: Reproduced with permission from Ref. 39.

Fig. 4. Schematic diagram of  $\text{Ce}_{2-x}\text{@HA}$  for co-enhancing PDT/PTT with SDT guided by NIR-II PA imaging.

harm DNA or organelles. Thus, X-rays can be utilized as an alternative light source for deep penetration (8–14 cm) into tissues.<sup>41</sup> Cerium-based doped nanoparticles have considerable application potential. Recently, researchers have doped Ce into  $\text{CaCO}_3$ ,  $\text{TiO}_2$ , etc., to build *in-vitro* and *in-vivo* models and activated PDT by using X-rays to generate ROS.

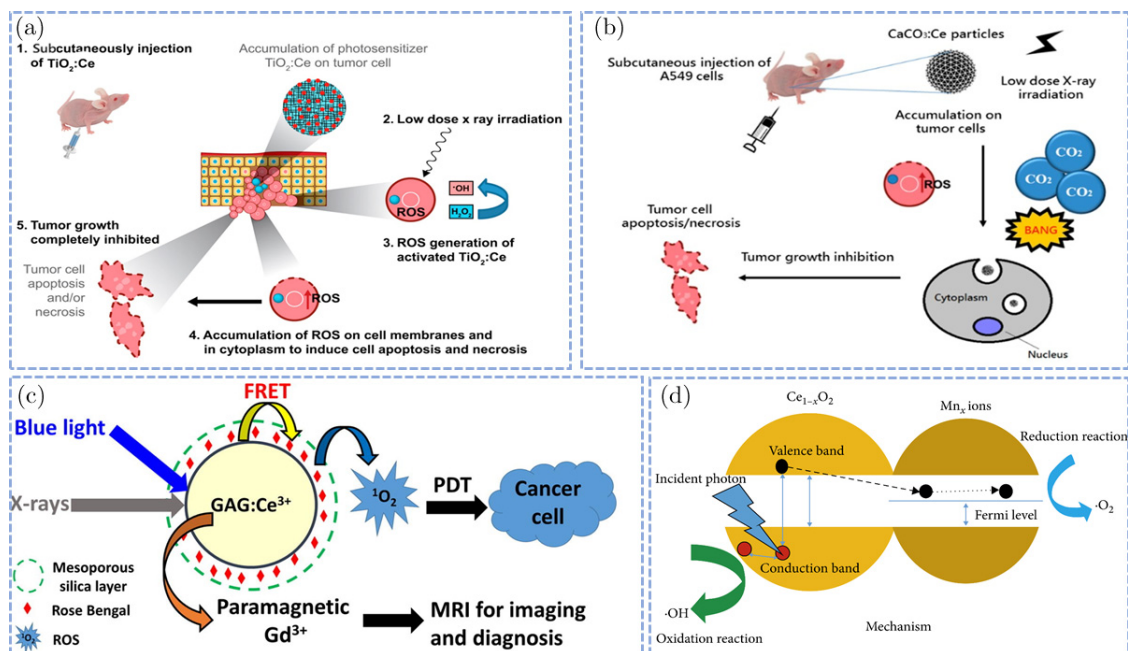
In 2017, Yang *et al.* reported that X-rays could activate Ce-doped  $\text{TiO}_2$  to act as a PS for PDT [Fig. 5(a)].  $\text{TiO}_2$  possesses the characteristics of low toxicity, good chemical stability, and high photocatalytic activity.<sup>42</sup> However, as a PS for cancer treatment,  $\text{TiO}_2$  still suffers from insufficient ROS production and a high required X-ray dose, resulting in a poor therapeutic effect. Doping Ce into  $\text{TiO}_2$  effectively narrows the energy gap and facilitates ROS generation.<sup>43</sup>

$\text{CaCO}_3$  is one of the main inorganic substances found in nature and has been utilized in medication delivery systems due to its excellent biocompatibility characteristics and low manufacturing cost.<sup>47</sup> In 2019, Yang *et al.* used coprecipitation to synthesize  $\text{Ce}:\text{CaCO}_3$  for use in oncotherapy [Fig. 5(b)].<sup>44</sup> The synthesized particles had a diameter of 100–300 nm and could be ingested by A549 cells through the endocytosis pathway. The {110} facet of cerium provided a strong photon interaction to absorb X-ray radiation, leading to the

overproduction of ROS.<sup>48</sup> A high ROS concentration can induce oxidative damage to mitochondrial proteins, DNA, and lipids, culminating in mitochondrial damage and death. Under acidic conditions,  $\text{CaCO}_3$  degraded and produced  $\text{CO}_2$ , which had an explosive effect that led to physical cell damage and even cell death.

The ability of X-rays to penetrate deeply into tissues has been boosted in deep-lying PDT cancers. For example, Wang *et al.* used mesoporous silica preloaded with  $\text{SrAl}_2\text{O}_4:\text{Eu}^{2+}$  NPs and an MC540 to perform X-PDT on H1299 cancers without side effects on normal tissues.<sup>49</sup> Among the numerous reports on the development of X-PDT nanocomposite systems, most use porphyrin derivatives for PDT, which often have limited spectral overlap with the donor (rare-earth-doped nanoscintillator) and reduce PDT efficacy. Jain *et al.* [Fig. 5(c)] reported a brand new multifunctional magnetic-luminescent  $\text{Gd}_{2.98}\text{Ce}_{0.02}\text{Al}_5\text{O}_{12}\text{@mSiO}_2\text{@RB}$  ( $\text{GAG@mSiO}_2\text{@RB}$ ).<sup>45</sup> Upon X-rays excitation,  $\text{GAG@mSiO}_2\text{@RB}$  NPs produced ROS efficaciously, demonstrating the development of a novel magnetic-luminescent nanoplatform that holds considerable promise for simultaneous detection and PDT of deeply buried cancers.

Furthermore,  $\text{Mn}_x\text{Ce}_{1-x}\text{O}_2$  nanoparticles were synthesized to explore their phototoxicities and antibacterial activities [Fig. 5(d)]. It was verified



Source: Reproduced with permission from Refs.42 and44-46.

Fig. 5. (a) The process of TiO<sub>2</sub>:Ce nanomaterial for tumor inhibition under low-dose X-ray irradiation. (b) CaCO<sub>3</sub>:Ce for synergistic CO<sub>2</sub> gas/X-ray-excited photodynamic therapy. (c) GAG@mSiO<sub>2</sub>@RB NPs for magnetic resonance imaging-guided deep PDT. (d) The interaction between Ce<sub>1-x</sub>O<sub>2</sub> and Mn<sub>x</sub>.

that 9% doped with CeO<sub>2</sub> exhibited a 40% inhibition of the bacterial growth of *Staphylococcus aureus*, a 46% inhibition against *Escherichia coli*, and a 44% inhibition against *Pseudomonas aeruginosa*. In addition, the survival rate of MCF-7 cancer cells decreased to 7.33% after PDT.<sup>46</sup>

### 3.3. Cerium-oxide-based inorganic composite nanoparticles

Chemotherapy remains the main treatment method for cancer. Despite numerous efforts, the performance of chemotherapy is hampered by poor drug accumulation at the cancer site and the prominent adverse effects of anticancer medicine on normal tissues. Therefore, it is necessary to develop targeted therapeutic nanoparticles to achieve cancer-specific enrichment while minimizing the adverse effects of anticancer drugs.

Previous studies indicated that CeO<sub>2</sub> can be cytotoxic to cancer cells through cell membrane damage and lipid peroxidation.<sup>50</sup> In addition, Ce(IV) can revert to Ce(III) in the acidic cancer microenvironment accompanied by ROS generation to achieve a synergistic therapeutic effect. For example, a delivery mechanism based on polydopamine

(PDA)-coated cerium oxide was developed for targeted PDT of human hepatoma HepG2 cells.<sup>51</sup>

A dense PDA layer was formed on cerium oxide nanorods (CeONR) by a dopamine self-polymerization process under alkaline circumstances. The surface of CeONR was then modified with thiolated galactose (Gal-SH) and hypericin (Hyp) to create CeONR@PDA-Gal/Hyp. The hypericin drug delivery system demonstrated excellent biocompatibility and selective targeting capabilities, with galactose units specifically recognizing overexpressed asialo-glycoprotein receptors (ASGP-R). MTT assay showed that the HepG2 viability was dropped (10–20%) at the concentration investigated under a dark condition, while the cell viability of 293T remained almost unchanged, indicating the negligible dark toxicity of CeONR@PDA-Gal/Hyp. After being taken up by HepG2 cells, CeONR@PDA-Gal/Hyp was able to execute PDT when exposed to a 590-nm laser.

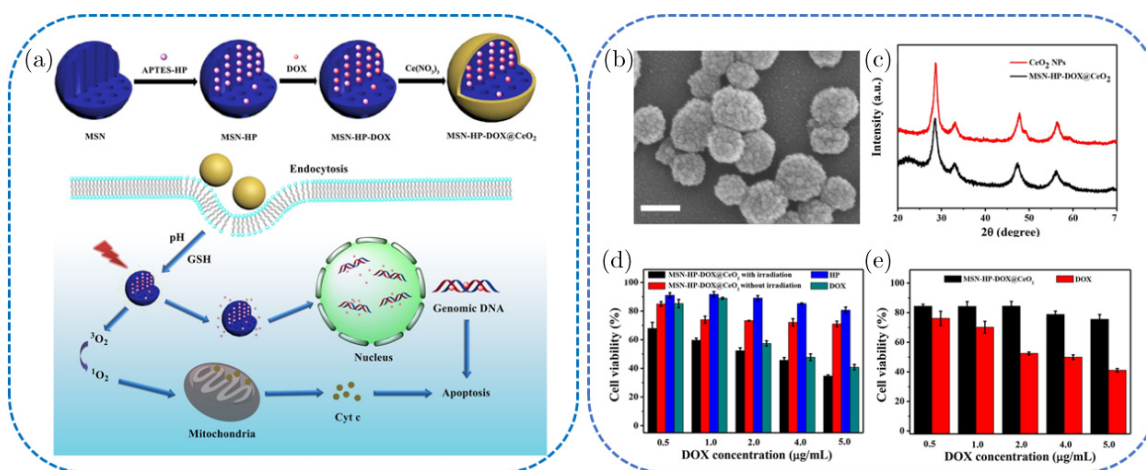
In addition, cerium oxide can be converted into Ce ions under reducing conditions.<sup>52</sup> CeO<sub>2</sub> NPs possess a strong fluorescence quenching capability that can be used to construct a “turn-on” fluorescent probe for real-time monitoring of drug release. For example, CeO<sub>2</sub>-coated mesoporous silica NPs

(MSN-HP-DOX@CeO<sub>2</sub>) were designed and prepared for combined chemotherapy and PDT [Fig. 6(a)].<sup>52</sup> Both hematoporphyrin (HP) and doxorubicin (DOX) possess conjugated structures that can be combined through  $\pi$ - $\pi$  interactions to facilitate DOX loading. Ingestion of MSN-HP-DOX@CeO<sub>2</sub> by cancer cells results in the reduction of CeO<sub>2</sub> NPs to Ce ions in an intracellular microenvironment with a high concentration of glutathione (GSH) and low pH. Figure 6(b) is a SEM image showing the spherical structure of MSN-HP-DOX@CeO<sub>2</sub>. Figure 6(c) shows XRD patterns confirming that CeO<sub>2</sub> was successfully coated on mesoporous silica nanoparticles (MSN). The release of DOX and the production of <sup>1</sup>O<sub>2</sub> led to a decrease in cell viability upon exposure to a 650-nm laser [Figs. 6(d) and 6(e)].

In another study, Xu *et al.* developed a novel therapeutic nanoplatform (DOX-Pt@CeO<sub>2</sub>@MnO<sub>2</sub>) for combined photothermal therapy/PDT/chemotherapy.<sup>53</sup> After Pt@CeO<sub>2</sub>@MnO<sub>2</sub> preloaded with DOX accumulated in a tumor, the protective layer of MnO<sub>2</sub> catalyzed intratumoral hydrogen peroxide to produce oxygen to enhance PDT and was degraded in the acidic environment to realize cancer-microenvironment-responsive release of DOX. Moreover, the introduction of Pt enhanced the separation of photogenerated electrons and holes, which facilitated <sup>1</sup>O<sub>2</sub> generation. HepG2 cells treated with DOX-Pt@CeO<sub>2</sub>@MnO<sub>2</sub> and 808 laser exhibit a remarkable decrease in cell activity. *In-vivo*

anticancer evaluation indicated that Pt@CeO<sub>2</sub>@MnO<sub>2</sub> produced an excellent anticancer effect through multimodal therapy with synthetic effects.

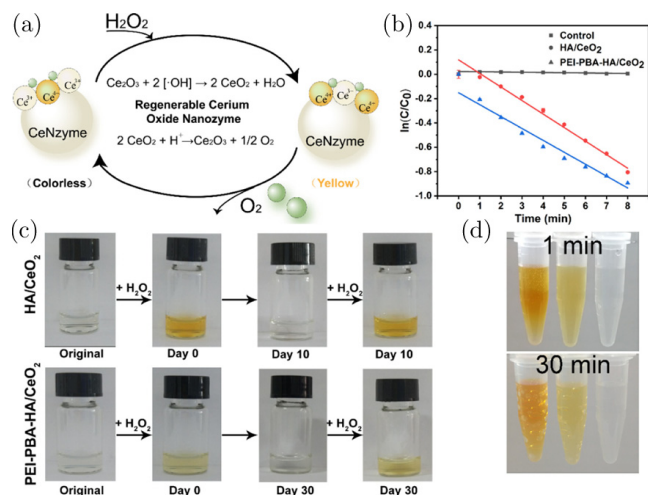
Currently, a variety of strategies have been explored to elevate the concentration of O<sub>2</sub> to improve PDT efficacy. For example, Liu *et al.* fabricated a multifunctional CeO<sub>2</sub>-PEG-Ce6-GoX (CPCG) to generate O<sub>2</sub>: high levels of hydrogen peroxide (H<sub>2</sub>O<sub>2</sub>) in the cancer microenvironment were converted to oxygen by making a great deal of the catalase-mimicking activity of CeO<sub>2</sub>, where PEG denotes phosphoethanolamine-polyethylene glycol with hydrophobic and hydrophilic and fragments,<sup>55</sup> Ce6 denotes Chlorin e6, GoX denotes glucose oxidase<sup>54,55</sup> Similarly, Zeng *et al.* reported<sup>56</sup> a double-targeted cancer medication delivery system (ICG@PEI-PBA-HA/CeO<sub>2</sub>) based on an inorganic nanozyme (CeO<sub>2</sub>), where PEI denotes polyethylenimine, PBA denotes 4-carboxylphenylboronic acid inacol ester, and HA denotes hyaluronate. Figure 7(a) is a schematic of the drug-loaded complex, showing the transition between the valence states of Ce(III) and Ce(IV), as well as the regenerable cycle of the cerium oxide nanozyme. The valence transition of cerium ions manifests as a change in the solution color [Fig. 7(b)]. ICG@PEI-PBA-HA/CeO<sub>2</sub> can catalyze H<sub>2</sub>O<sub>2</sub> to O<sub>2</sub> at various concentrations [Figs. 7(c) and 7(d)]. ICG@PEI-PBA-HA/CeO<sub>2</sub> significantly relieved hypoxia inside cancer *in vivo*, thereby efficiently enhancing PDT.



Source: Reproduced with permission from Ref. 52.

Fig. 6. (a) Schematic illustration of a synthetic methodology for a triple-stimulus-responsive medication delivery system. (b) SEM images of MSN-HP-DOX@CeO<sub>2</sub>. Scale bar: 100 nm. (c) XRD patterns of CeO<sub>2</sub> NPs, as well as MSN-HP-DOX@CeO<sub>2</sub>. (d) MSN-HP-DOX@CeO<sub>2</sub> cytotoxicity values on HeLa cells for 24 h with and without radiation and with HP and DOX at varying doses. (e) Cytotoxicity values for 24 h of MSN-HP-DOX@CeO<sub>2</sub> and DOX at various doses on 293T cells.





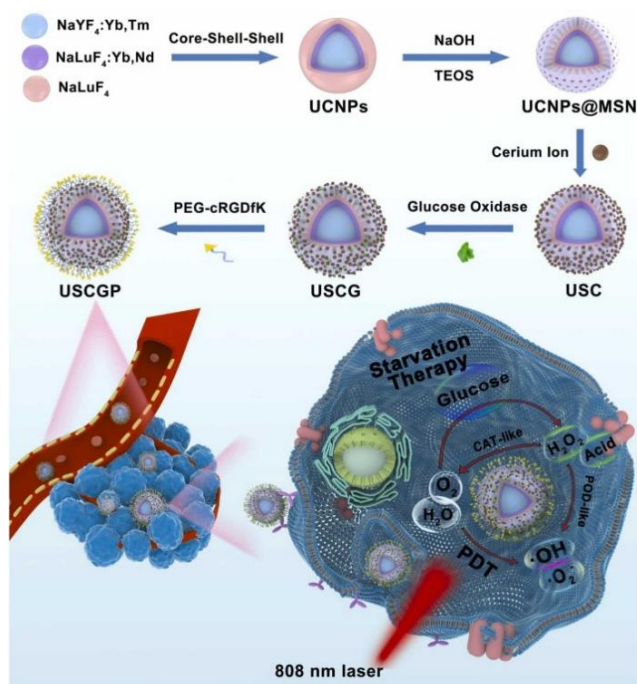
Source: Reproduced with permission from Ref. 56.

Fig. 7. (a) Diagram illustrating the catalase activities of HA/CeO<sub>2</sub> and PEI-PBA-HA/CeO<sub>2</sub>, as well as the regeneration cycle of CeO<sub>2</sub> and the crossover between its valence states. (b) Evaluation of the cerium oxide nanozyme's catalytic activity. (c) Cerium oxide regeneration cycle: temporal color shift in the samples reveals the transformation between Ce(III) and Ce(IV). (d) Oxygen generation caused by the catalysis of H<sub>2</sub>O<sub>2</sub> at different HA/CeO<sub>2</sub> concentrations.

In 2022, Gao *et al.* designed a multilayered porous biocatalyst to realize cascade synergistic cancer therapy.<sup>57</sup> First, the researchers synthesized OA-stabilized core-shell-shell-structured NaYF<sub>4</sub>:Yb,Tm@NaLuF<sub>4</sub>:Yb,Nd@NaLuF<sub>4</sub> NPs (UCNPs). And then MSN, CeO<sub>2</sub>, and glucose oxidase (GOD) were modified in turn on the exterior of UCNPs to construct UCNPs@mSiO<sub>2</sub>@CeO<sub>2</sub>-GOD (USCG). Finally, USCGP was harvested after using PEG-cRGDFK to modify the surface of USCG. In this system, GOD catalyzes the decomposition of glucose and simultaneously regulates the tumor environment (TME), activating the catalysis of USCGP (Fig. 8). Moreover, the cascade interactions between GOD and CeO<sub>2</sub> accelerate the generation of •OH and accelerate nutrient depletion in TME. Experimentally, USCGP with good biocompatibility exhibited efficient elimination of cancer cells by a combination of PDT, chemodynamic therapy, and starvation therapy.

### 3.4. Cerium-oxide-based organic composite nanoparticles

The ROS production levels of most PDT nanoparticles do not change with the disease microenvironment, which may limit selective treatment



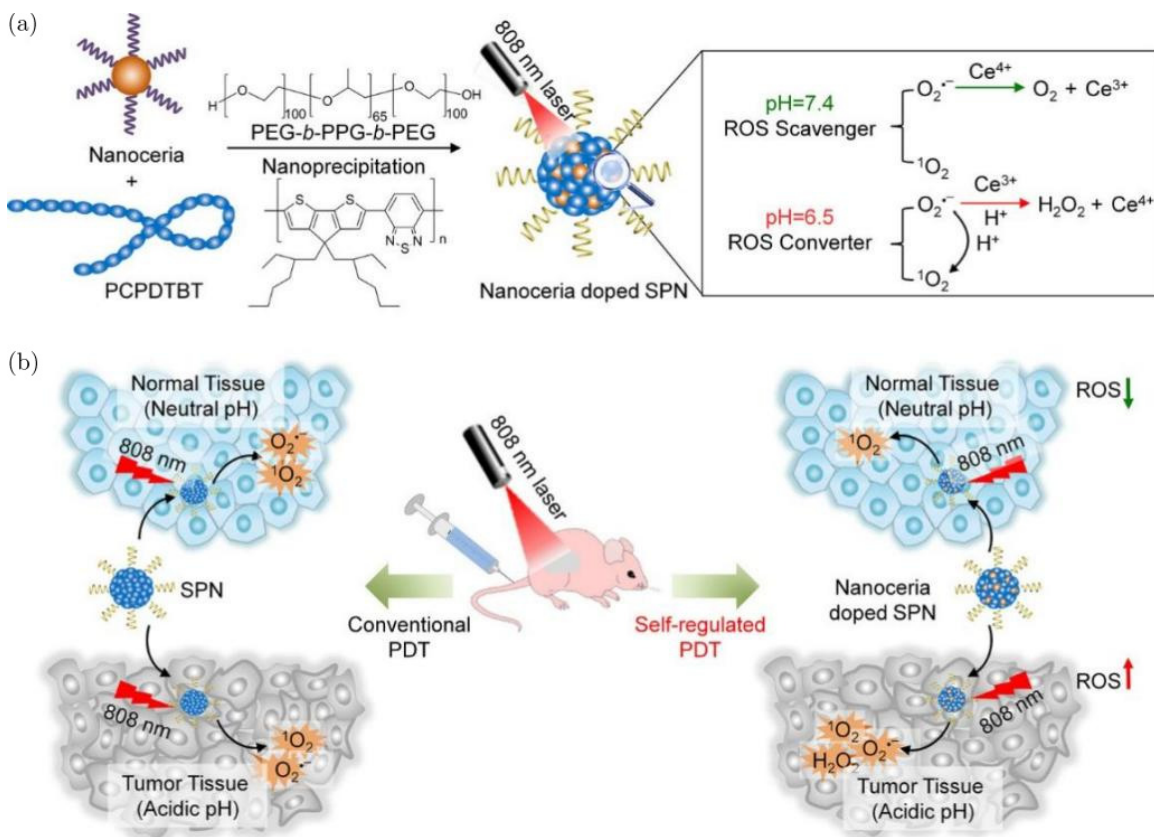
Source: Reproduced with permission from Ref. 57.

Fig. 8. The preparation and cascade-reaction process of USCGP biocatalyst for synergistic starvation/PDT cancer treatment.

using these nanoparticles due to potential damage to normal tissues. Recently, Hu and Ding reported a simple pH/H<sub>2</sub>O<sub>2</sub>-activatable, O<sub>2</sub>-evolving, and ROS-regulating DOX and ICG co-loading PEGylated polyaniline (PANI)-coated CeO<sub>x</sub>@polyacrylic acid (PAA) nanoclusters, PAA-CeO<sub>x</sub>@PANI-PEG nanoclusters (CPs), for cancer combination treatment.<sup>58</sup> Depending on the dual-mode catalytic characteristics of Ce at varying pH, it operates as catalase-like catalytic agents (pH = 7.4–6.5, Ce<sup>4+</sup>/Ce<sup>3+</sup> = 3.46), and as oxidase-like catalytic agents (pH = 5.4–6.5, Ce<sup>4+</sup>/Ce<sup>3+</sup> = 0.58),<sup>59,60</sup> which is able to increase the intracellular O<sub>2</sub> and ROS levels in cancer region. In addition, due to the protective effect of PAA, PANI, and PEG, the catalase activity of CeO<sub>x</sub> would be activated upon irradiation with NIR light after accumulation at the tumor site.

Semiconducting polymer nanoparticles (SPNs) are a novel type of molecular imaging and PDT nanoagent that circumvents the potential toxicity of metal ions and possesses intrinsically good biocompatibility.<sup>61</sup> Zhu *et al.* reported a hybrid approach for modulating the PDT properties of SPNs to optimize cancer therapy.<sup>62</sup> SPNs have two active components (Fig. 9): CeO<sub>2</sub> NPs and poly





Source: Reproduced with permission from Ref. 62.

Fig. 9. Schematic diagrams of (a) the formation of nanoceria-doped SPNs, as well as the self-regulating PDT properties of SPNs in physiologically neutral and pathologically acidic environments, and (b) nanoceria-doped SPNs versus nondoped SPNs as mediators of self-regulated and conventional PDT.

(cyclopentadithiophene-alt-benzothiadiazole) (PCPDTBT). CeO<sub>2</sub> NPs were easily doped into PCPDTBT nanoparticles by nanoprecipitation. PCPDTBT has triple energy of 1 eV,<sup>63</sup> which exceeds the energy gap between O<sub>2</sub> and <sup>1</sup>O<sub>2</sub> (0.98 eV) and is therefore theoretically feasible for cancer PDT. Due to a dense concentration of surface oxygen vacancies, nanoceria may alternate between the oxidation states of Ce(III) and Ce(IV) depending on the pH. As a result, combining CeO<sub>2</sub> NPs and PCPDTBT NPs can significantly amplify anticancer effects in an acidic cancer microenvironment while reducing the side effects on normal tissues.

The different effects of Ce under neutral and acidic conditions determine the underlying mechanism of pH-dependent PDT. The presence of reduced-state Ce(III) and oxidized-state Ce(IV) facilitates the antioxidant action of nanoceria, which can extinguish ROS under neutral circumstances while converting O<sub>2</sub><sup>•-</sup> to H<sub>2</sub>O<sub>2</sub> to generate

ROS under acidic conditions.<sup>62</sup> In addition, H<sub>2</sub>O<sub>2</sub> can generate more ROS, including •OH, hypochlorite (OCl<sup>-</sup>), or hypobromite (OBr<sup>-</sup>), using metal-catalyzed Fenton reactions and peroxidase-catalyzed reactions.<sup>64</sup> There have been many reports that high levels of H<sub>2</sub>O<sub>2</sub> are more detrimental to cellular equilibrium than high concentrations of O<sub>2</sub><sup>•-</sup>.<sup>65,66</sup> These integrated effects ultimately result in an increase in total ROS generation under pathologically acidic settings and a reduction under physiologically neutral ones. This study introduces a hybrid optical approach to modulate nanotheranostic agents based on organic SPNs and nanoceria and provides alternative design guidelines for PDT.

#### 4. Future Perspective

PDT is a ROS-induced local therapy with excellent efficacy for cancer treatment. The PDT function depends on the effect of light, PSs, and O<sub>2</sub>.<sup>67</sup>

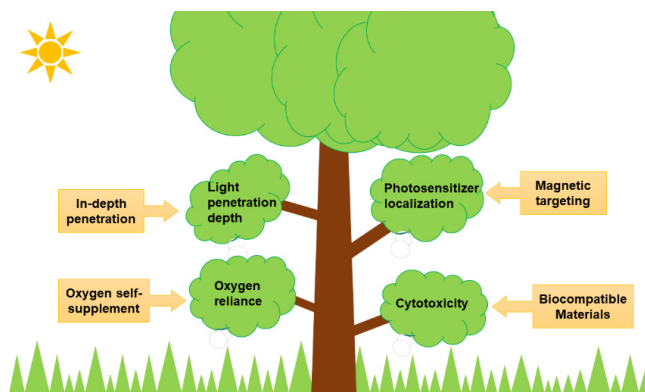


Fig. 10. Schematic diagram of challenges that the conventional PDT processes have encountered at different levels, as well as the advanced strategies to solve these matters.

However, there are still some serious challenges for PDT (Fig. 10), as follows: (i) the development of highly effective and nontoxic or low cytotoxic PSs; (ii) the light penetration depth that severely impairs the application of photodynamic therapy to epidermal cancers (e.g., oral cancer, skin cancer, and bowel lesions<sup>42</sup>); (iii) oxygen dependence compromising the effectiveness of PDT against hypoxic cancers; and (iv) continuing difficulties with the delivery and the clearance of exogenous PSs.

Zhang *et al.* found negligible cytotoxicity for CeO<sub>2</sub> NPs.<sup>22</sup> Furthermore, CeO<sub>2</sub> NPs exhibit different enzyme-like activities in different physiological environments; for example, CeO<sub>2</sub> NPs can scavenge ROS in normal cells but not in cancer cells and can thereby be used for the specific treatment of cancers. One of the current challenges for PDT is the development of biocompatible PSs to minimize potential biotoxicity. From this perspective, the exploitation of cerium-based PSs have exceptional application prospects.

The light penetration depth is a barrier to using PDT for deep-tissue cancer. X-rays are a light source with considerable promise because of the absence of tissue penetration restrictions. Therefore, Albuquerque *et al.* designed and synthesized cerium-based hybrid materials (CeO<sub>x</sub>/TiO<sub>2</sub>) and used the {110} face of Ce to absorb X-ray radiation to successfully implement deep-tissue PDT.<sup>43</sup>

In addition, poor accumulation of PSs in cancers limits therapeutic efficacy. Cerium-based magnetic hybrid materials could be used to ameliorate this drawback.<sup>68</sup> For example, Wang *et al.* exploited the magnetic property of citrate–Ce complexes to construct a multifunctional nanoplatform

(AuNR@SiO<sub>2</sub>/Ce@Dox@polydopamine@aptamer) for dual-targeted therapy of non-small-cell lung cancer. *In-vitro* anticancer studies indicated that the adhibition of a magnetic field enhanced the anticancer effect of AuNR@SiO<sub>2</sub>/Ce@Dox@ polydopamine@ aptamer on A549 cells.<sup>69</sup>

The enzymatic properties (superoxide-dismutase-like and catalase-like activities) of CeO<sub>2</sub> and cancer microenvironment characteristics can be utilized to convert high concentrations of ROS (such as O<sub>2</sub><sup>•-</sup> and H<sub>2</sub>O<sub>2</sub>) into oxygen,<sup>54</sup> thereby increasing the content of endogenous oxygen and achieving oxygen self-supplementation. Based on the unique physicochemical properties of cerium-based nanoparticles, we have full confidence in the expansion of cancer treatment options from the rational design of PDT strategies. However, most revealed PDT treatments are still in the early stage because of a lack of clinical evidence. The *in-vivo* biological effects of cerium-based nanoparticles should be investigated in the future. Finally, we hope that this review provides a timely overview of cerium-based PDT that opens up a new avenue in the future for the ongoing fight against cancer.

## Conflict of Interest

The authors declare no conflict of interest.

## Acknowledgments

This work was supported by the National Natural Science Foundation (NNSF) of China (52103166 and 61935004), the Natural Science Foundation (NSF) of Jiangsu Province (BK20200710), Jiangsu Postdoctoral Science Foundation (51204087), NSF of Shandong Province (ZR2020KB018), “Taishan Scholars” Construction Special Fund of Shandong Province, the Natural Science Foundation of Ningbo (202003N40448), and the Open Project Program of Wuhan National Laboratory for Optoelectronics No. 2020WNLOKF022.

## References

1. G. Lan, K. Ni, W. Lin, “Nanoscale metal–organic frameworks for phototherapy of cancer,” *Coord. Chem. Rev.* **379**, 65–81 (2017).
2. P. Cai, W. Yang, Z. He, H. Jia, H. Wang, W. Zhao, “A chlorin-lipid nanovesicle nucleus drug for

- amplified therapeutic effects of lung cancer by internal radiotherapy combined with the Cerenkov radiation-induced photodynamic therapy,” *Biomater. Sci.* **8**, 4841–4851 (2020).
3. H. S. Walter, S. I. Ahmed, “Targeted therapies in cancer,” *Surgery (Oxford)* **39**(4), 202–207 (2021).
  4. D. Yang, X. Lv, L. Xue, N. Yang, “A lipase-responsive antifungal nanoplatform for synergistic photodynamic/photothermal/pharmaco-therapy of azole-resistant *Candida albicans* infections,” *Chem. Commun.* **55**(100), 15145–15148 (2019).
  5. D. Yang, L. Sun, L. Xue, X. Wang, Y. Hu, J. Shao, L. Fu, X. Dong, “Orthogonal Aza-BODIPY–BODIPY dyad as heavy-atom free photosensitizer for photo-initiated antibacterial therapy,” *J. Innov. Opt. Health Sci.* **15**(1), 2250004 (2022).
  6. C. Cao, T. Zhang, N. Yang, X. Niu, Z. Zhou, J. Wang, D. Yang, P. Chen, L. Zhong, X. Dong, “POD Nanozyme optimized by charge separation engineering for light/pH activated bacteria catalytic/photodynamic therapy,” *Signal Transduct. Target. Ther.* **7**(1), 86 (2022).
  7. D. Chen, Z. Zhong, Q. Ma, J. Shao, W. Huang, X. Dong, “Aza-BODIPY-based nanomedicines in cancer phototheranostics,” *ACS Appl. Mater.* **12**(24), 26914–26925 (2020).
  8. X. Dai, T. Du, K. Han, “Engineering nanoparticles for optimized photodynamic therapy,” *ACS Biomater. Sci. Eng.* **5**(12), 6342–6354 (2019).
  9. H. Dai, Z. Cheng, T. Zhang, W. Wang, J. Shao, W. Wang, Y. Zhao, X. Dong, L. Zhong, “Boron difluoride formazanate dye for high-efficiency NIR-II fluorescence imaging-guided cancer photothermal therapy,” *Chin. Chem. Lett.* **33**(5), 2501–2506 (2021).
  10. W. K. Ong, X. Yao, D. Jana, M. Li, Y. Zhao, Z. Luo, “Efficient production of reactive oxygen species from Fe<sub>3</sub>O<sub>4</sub>/ZnPC coloaded nanoreactor for cancer therapeutics in vivo,” *Small Struct.* **1**(3), 2000065 (2020).
  11. J. Yan, X. Zhan, Z. Zhang, K. Chen, M. Wang, Y. Sun, B. He, Y. Liang, “Tetrahedral DNA nanostructures for effective treatment of cancer: Advances and prospects,” *J. Nanobiotechnol.* **19**(1), 412 (2021).
  12. B. Joseph, V. Sagarika, C. Sabu, N. Kalarikkal, S. Thomas, “Cellulose nanocomposites: Fabrication and biomedical applications,” *J. Bioresour. Bioprod.* **5**(4), 223–237 (2020).
  13. M. R. Saeb, N. Rabiee, F. Seidi, B. F. Far, M. Bagherzadeh, E. C. Lima, M. Rabiee, “Green CoNi<sub>2</sub>S<sub>4</sub>/porphyrin decorated carbon-based nanocomposites for genetic materials detection,” *J. Bioresour. Bioprod.* **6**(3), 215–222 (2021).
  14. D. Yang, F. Chen, S. He, H. Shen, Y. Hu, N. Feng, S. Wang, L. Weng, Z. Luo, L. Wang, “One-pot growth of triangular SnS nanopyramids for photoacoustic imaging and photothermal ablation of tumors,” *New J. Chem.* **43**(33), 13256–13262 (2019).
  15. W. Xiu, S. Gan, Q. Wen, “Biofilm microenvironment-responsive nanotheranostics for dual-mode imaging and hypoxia-relief-enhanced photodynamic therapy of bacterial infections,” *Research* **2020**, 9426453 (2020).
  16. W. Xu, X. Qing, S. Liu, D. Yang, X. Dong, Y. Zhang, “Hollow mesoporous manganese oxides: Application in cancer diagnosis and therapy,” *Small* **18**(15), 2106511 (2022).
  17. C. Cao, H. Zou, N. Yang, H. Li, Y. Cai, X. Song, J. Shao, P. Chen, X. Mou, W. Wang, “Fe<sub>3</sub>O<sub>4</sub>/Ag/Bi<sub>2</sub>MoO<sub>6</sub> photoactivatable nanozyme for self-replenishing and sustainable cascaded nanocatalytic cancer therapy,” *Adv. Mater.* **33**(52), 2106996 (2021).
  18. D. Jampaiah, T. Srinivasa Reddy, A. E. Kandjani, P. R. Selvakannan, Y. M. Sabri, V. E. Coyle, R. Shukla, S. K. Bhargava, “Fe-doped CeO<sub>2</sub> nanorods for enhanced peroxidase-like activity and their application towards glucose detection,” *J. Mater. Chem. B* **4**(22), 3874–3885 (2016).
  19. Y. Duygu, G. Burcu, B. Esra, K. Çiğdem, M. C. Demir, T. Ali, “A new nanozyme with peroxidase-like activity for simultaneous phosphoprotein isolation and detection based on metal oxide affinity chromatography: Monodisperse-porous cerium oxide microspheres,” *Chem. Eng. J.* **403**, 126357 (2020).
  20. Q. Ma, X. Sun, W. Wang, D. Yang, C. Yang, Q. Shen, J. Shao, “Diketopyrrolopyrrole-derived organic small molecular dyes for tumor phototheranostics,” *Chin. Chem. Lett.* **33**(4), 1681–1692 (2021).
  21. H. Dai, X. Wang, J. Shao, W. Wang, X. Mou, X. Dong, “NIR-II organic nanotheranostics for precision oncology,” *Small* **17**(44), 2102646 (2021).
  22. L. Zhang, H. Jiang, M. Selke, X. Wang, “Selective cytotoxicity effect of cerium oxide nanoparticles under UV irradiation,” *J. Biomed. Nanotechnol.* **10**(9), 278–286 (2014).
  23. E. Shoko, M. F. Smith, R. H. McKenzie, “Charge distribution near bulk oxygen vacancies in cerium oxides,” *J. Phys., Condens. Matter* **22**(22), 223201 (2010).
  24. Z. Tian, T. Yao, C. Qu, S. Zhang, X. Li, Y. Qu, “Photolyase-like catalytic behavior of CeO<sub>2</sub>,” *Nano Lett.* **19**, 8270–8277 (2019).
  25. Z. Wang, L. Fu, Y. Zhu, S. Wang, G. Shen, L. Jin, R. Liang, “Chemodynamic/photothermal synergistic

- therapy based on Ce-doped Cu–Al layered double hydroxides,” *J. Mater. Chem. B* **9**, 710–718 (2020).
26. Y. Yan, Y. Hou, H. Zhang, W. Gao, R. Han, J. Yu, L. Xu, K. Tang, “CeO<sub>2</sub> QDs anchored on MnO<sub>2</sub> nanoflowers with multiple synergistic effects for amplified tumour therapy,” *Colloids Surf. B, Biointerfaces* **208**, 112103 (2021).
  27. G. Vinothkumar, I. L. Arun, K. S. Babu, “Cerium phosphate–cerium oxide heterogeneous composite nanozymes with enhanced peroxidase-like biomimetic activity for glucose and hydrogen peroxide sensing,” *Inorg. Chem.* **58**, 349–358 (2018).
  28. Y. Yue, H. Wei, J. Guo, Y. Yang, “Ceria-based peroxidase-mimicking nanozyme with enhanced activity: A coordination chemistry strategy,” *Colloids Surf. A, Physicochem. Eng. Aspects* **610**, 125715 (2021).
  29. R. Imran, O. Girgis, B. Shazia, H. Tayyaba, K. David, “Photodynamic therapy: Promoting in vitro efficacy of photodynamic therapy by liposomal formulations of a photosensitizing agent,” *Lasers Surg. Med.* **50**, 499–505 (2018).
  30. Y. Liang, L. Lu, Y. Chen, Y. Lin, “Photodynamic therapy as an antifungal treatment,” *Exp. Ther. Med.* **12**, 23–27 (2016).
  31. J. Liu, L. Ye, W. Xiong, T. Liu, H. Yang, J. Lei, “A cerium oxide@metal–organic framework nanoenzyme as a tandem catalyst for enhanced photodynamic therapy,” *Chem. Commun.* **57**, 2820–2823 (2021).
  32. A. Heidi, R. H. Michael, “New photosensitizers for photodynamic therapy,” *Biochem. J.* **473**(4), 347–364 (2016).
  33. L. Lin, X. Song, X. Dong, B. Li, “Nanophotosensitizers for enhanced photodynamic therapy,” *Photodiagnosis Photodyn. Ther.* **31**, 102597 (2021).
  34. M. Zhang, C. Zhang, X. Zhai, F. Luo, Y. Du, C. Yan, “Antibacterial mechanism and activity of cerium oxide nanoparticles,” *Sci. China Mater.* **62**(11), 1727–1739 (2019).
  35. Y. Chang, Y. Feng, Y. Cheng, R. Zheng, X. Wu, H. Jian, “Anisotropic plasmonic metal heterostructures as theranostic nanosystems for near infrared light-activated fluorescence amplification and phototherapy,” *Adv. Sci.* **6**, 1900158 (2019).
  36. M. Qi, W. Li, X. Zheng, X. Li, Y. Sun, Y. Wang, C. Li, L. Wang, “Cerium and its oxidant-based nanomaterials for antibacterial applications: A state-of-the-art review,” *Front. Mater.* **7**, 213 (2020).
  37. Z. Tian, X. Li, Y. Ma, T. Chen, D. Xu, “Quantitatively intrinsic biomimetic catalytic activity of nanocerias as radical scavengers and their ability against H<sub>2</sub>O<sub>2</sub> and doxorubicin-induced oxidative stress,” *ACS Appl. Mater. Interfaces* **9**(28), 23342–23352 (2017).
  38. S. Clement, W. Deng, E. Camilleri, B. C. Wilson, E. M. Goldys, “X-ray induced singlet oxygen generation by nanoparticle-photosensitizer conjugates for photodynamic therapy: Determination of singlet oxygen quantum yield,” *Sci. Rep.* **6**, 19954 (2016).
  39. J. Li, H. Peng, C. Wen, P. Xu, X. Shen, C. Gao, “NIR-II-responsive CeO<sub>2-x</sub>@HA nanotheranostics for photoacoustic imaging-guided sonodynamic-enhanced synergistic phototherapy,” *Langmuir* **38**(18), 5502–5514 (2022).
  40. X. Han, J. Huang, X. Jing, D. Yang, H. Lin, Z. Wang, P. Li, Y. Chen, “Oxygen-deficient black titania for synergistic/enhanced sonodynamic and photoinduced cancer therapy at near infrared-II biowindow,” *ACS Nano* **12**(5), 4545–4555 (2018).
  41. J. D. Carter, N. N. Cheng, Y. Qu, G. D. Suarez, T. Guo, “Nanoscale energy deposition by X-ray absorbing nanostructures,” *J. Phys. Chem. B* **111**(40), 11622–11625 (2007).
  42. C. Yang, Y. Sun, P. Chung, W. Chen, “Development of Ce-doped TiO<sub>2</sub> activated by X-ray irradiation for alternative cancer treatment,” *Ceram. Int.* **15**, 12675–12683 (2017).
  43. R. A. Anderson, B. Albert, R. S. Julio, I. Francesc, “Theoretical study of the stoichiometric and reduced Ce-doped TiO<sub>2</sub> anatase (001) surfaces,” *J. Phys. Chem. C* **119**, 4805–4816 (2015).
  44. C. Yang, W. Wang, F. Lin, C. Hou, “Rare-earth-doped calcium carbonate exposed to X-ray irradiation to induce reactive oxygen species for tumor treatment,” *Int. J. Mol. Sci.* **20**(5), 1148 (2019).
  45. A. Jain, R. Koyani, C. Munoz, P. Sengar, O. E. Contreras, P. Juarez, G. A. Hirata, “Magnetic-luminescent cerium-doped gadolinium aluminum garnet nanoparticles for simultaneous imaging and photodynamic therapy of cancer cells,” *J. Colloid Interface Sci.* **526**, 220–229 (2018).
  46. M. Atif, I. Seemab, M. Fakhar-E-Alam, M. Ismail, M. Qaisar, M. Lubna, A. M. Hammad, H. Atif, W. A. Farooq, “Manganese-doped cerium oxide nanocomposite induced photodynamic therapy in MCF-7 cancer cells and antibacterial activity,” *BioMed Res. Int.* **2019**, 7156828 (2019).
  47. J. Zhu, A. Jiao, Q. Li, X. Lv, X. Wang, X. Song, B. Li, Y. Zhang, X. Dong, “Mitochondrial Ca<sup>2+</sup>-overloading by oxygen/glutathione depletion-boosted photodynamic therapy based on a CaCO<sub>3</sub> nanopatform for tumor synergistic therapy,” *Acta Biomater.* **137**, 252–261 (2021).
  48. L. Huang, W. Zhang, K. Chen, W. Zhu, X. Liu, “Facet-selective response of trigger molecule to CeO<sub>2</sub>{110} for up-regulating oxidase-like activity,” *Chem. Eng. J.* **330**, 746–752 (2017).
  49. G. D. Wang, H. T. Nguyen, H. Chen, P. B. Cox, L. Wang, K. Nagata, Z. Hao, A. Wang, Z. Li, J. Xie,



- “X-ray induced photodynamic therapy: A combination of radiotherapy and photodynamic therapy,” *Theranostics* **6**(13), 2295–2305 (2016).
50. L. Zhang, H. Zhong, H. Zhang, C. Ding, “A multifunctional nano system based on DNA and CeO<sub>2</sub> for intracellular imaging of miRNA and enhancing photodynamic therapy,” *Talanta* **221**, 121554 (2021).
  51. Y. Wang, Y. Zhang, M. Jin, Y. Lv, Z. Pei, Y. Pei, “A hypericin delivery system based on polydopamine coated cerium oxide nanorods for targeted photodynamic therapy,” *Polymers (Basel)* **11**(6), 1025 (2019).
  52. J. Wen, K. Yang, Y. Xu, H. Li, F. Liu, S. Sun, “Construction of a triple-stimuli-responsive system based on cerium oxide coated mesoporous silica nanoparticles,” *Sci. Rep.* **6**, 38931 (2016).
  53. Q. Xu, D. Li, H. Zhou, B. Chen, J. Wang, S. Wang, A. Chen, N. Jiang, “MnO<sub>2</sub>-coated porous Pt@CeO<sub>2</sub> core-shell nanostructures for photoacoustic imaging-guided tri-modal cancer therapy,” *Nanoscale* **13**, 16499–16508 (2021).
  54. X. Liu, J. Liu, S. Chen, Y. Xie, Q. Fan, “Dual-path modulation of hydrogen peroxide to ameliorate hypoxia for enhancing photodynamic/starvation synergistic therapy,” *J. Mater. Chem. B* **8**, 9933–9942 (2020).
  55. N. Li, Z. Duan, L. Wang, C. Guo, H. Zhang, Z. Gu, Q. Gong, K. Luo, “An amphiphilic PEGylated peptide dendron-gemcitabine prodrug-based nanoagent for cancer therapy,” *Macromol. Rapid Commun.* **42**(12), 2100111 (2021).
  56. L. Zeng, H. Cheng, Y. Dai, Z. Su, C. Wang, “In vivo regenerable cerium oxide nanozyme-loaded pH/H<sub>2</sub>O<sub>2</sub>-responsive nanovesicle for tumor-targeted photothermal and photodynamic therapies,” *ACS Appl. Mater. Interfaces* **13**(1), 233–244 (2020).
  57. X. Gao, J. Feng, S. Song, K. Liu, K. Du, Y. Zhou, K. Lv, H. Zhang, “Tumor-targeted biocatalyst with self-accelerated cascade reactions for enhanced synergistic starvation and photodynamic therapy,” *Nano Today* **43**, 101433 (2022).
  58. Z. Hu, Y. Ding, “Cerium oxide nanoparticles-mediated cascade catalytic chemo-photo tumor combination therapy,” *Nano Res.* **15**(1), 333–345 (2022).
  59. S. Dong, Y. Dong, T. Jia, S. Liu, J. Liu, D. Yang, F. He, S. Gai, P. Yang, J. Lin, “GSH-depleted nanozymes with hyperthermia-enhanced dual enzyme-mimic activities for tumor nanocatalytic therapy,” *Adv. Mater.* **32**(42), 2002439 (2020).
  60. S. Dong, Y. Dong, B. Liu, J. Liu, S. Liu, Z. Zhao, W. Li, B. Tian, R. Zhao, F. He, “Guiding transition metal-doped hollow cerium tandem nanozymes with elaborately regulated multi-enzymatic activities for intensive chemodynamic therapy,” *Adv. Mater.* **34**(7), 2107054 (2022).
  61. X. Lin, Y. Hu, C. Zhang, J. Yin, R. Cui, D. Yang, B. Chen, “More severe toxicity of gold nanoparticles with rougher surface in mouse hippocampal neurons,” *J. Central South Univ.* **28**(12), 3642–3653 (2021).
  62. H. Zhu, Y. Fang, Q. Miao, X. Qi, D. Ding, P. Chen, K. Pu, “Regulating near-infrared photodynamic properties of semiconducting polymer nanotheranostics for optimized cancer therapy,” *ACS Nano* **11**(9), 8998–9009 (2017).
  63. D. D. Nuzzo, A. Aguirre, M. Shahid, V. S. Gevaerts, S. C. Meskers, R. A. Janssen, “Improved film morphology reduces charge carrier recombination into the triplet excited state in a small bandgap polymer-fullerene photovoltaic cell,” *Adv. Mater.* **22**(38), 4321–4324 (2010).
  64. C. Winterbourn, “Reconciling the chemistry and biology of reactive oxygen species,” *Nat. Chem. Biol.* **4**(5), 278–286 (2008).
  65. I. Celardo, J. Z. Pedersen, E. Traversa, L. Ghibelli, “Pharmacological potential of cerium oxide nanoparticles,” *Nanoscale* **3**(4), 1411–1420 (2011).
  66. B. C. Nelson, M. E. Johnson, M. L. Walker, K. R. Riley, C. M. Sims, “Antioxidant cerium oxide nanoparticles in biology and medicine,” *Antioxidants* **5**(2), 15 (2016).
  67. Z. Zhou, J. Song, L. Nie, X. Chen, “Reactive oxygen species generating systems meeting challenges of photodynamic cancer therapy,” *Chem. Soc. Rev.* **45**(23), 6597–6626 (2016).
  68. Q. Yu, Z. Wei, X. Qin, L. Qin, Y. Li, J. Shi, D. Niu, “Reductant-free synthesis of MnO<sub>2</sub> nanosheet-decorated hybrid nanoplatfor for magnetic resonance imaging-monitored tumor microenvironment-responsive chemodynamic therapy and near-infrared-mediated photodynamic therapy,” *Small Struct.* **2**(12), 2100116 (2021).
  69. Y. Wang, L. Wang, L. Guo, M. Yan, “Photo-responsive magnetic mesoporous silica nanocomposites for magnetic targeted cancer therapy,” *New J. Chem.* **43**, 4908–4918 (2019).